JACS
JOURNAL OF THE AMERICAN CHEMICAL SOCIETY
Article
pubs.acs.org/JACS

Probing Site-Specific Structural Information of Peptides at Model Membrane Interface In Situ

Bei Ding,[†] Afra Panahi,[†] Jia-Jung Ho,[‡] Jennifer E. Laaser,[‡] Charles L. Brooks III,[†] Martin T. Zanni,*[,‡] and Zhan Chen*[,†]

[†]Department of Chemistry, University of Michigan, Ann Arbor, Michigan 48109, United States
[‡]Department of Chemistry, University of Wisconsin−Madison, Madison, Wisconsin 53703, United States

Supporting Information

ABSTRACT: Isotope labeling is a powerful technique to probe detailed structures of biological molecules with a variety of analytical methods such as NMR and vibrational spectroscopies. It is important to obtain molecular structural information on biological molecules at interfaces such as cell membranes, but it is challenging to use the isotope labeling method to study interfacial biomolecules. Here, by individually $^{13}C{=}^{16}O$ labeling ten residues of a peptide, Ovispirin-1, we have demonstrated for the first time that a site-specific environment of membrane associated peptide can be probed by the submonolayer surface sensitive sum frequency generation (SFG) vibrational spectroscopy in situ. With the peptide associated with a single lipid bilayer, the sinusoidal trend of the SFG line width and peak-center frequency suggests that the peptide is located at the interface beneath the lipid headgroup region. The constructive interferences between the isotope labeled peaks and the main peptide amide I peak contributed by the unlabeled components were used to determine the membrane orientation of the peptide. From the SFG spectral peak-center frequency, line width, and polarization dependence of the isotope labeled units, we deduced structural information on individual units of the peptide associated with a model cell membrane. We also performed molecular dynamics (MD) simulations to understand peptide−membrane interactions. The physical pictures described by simulation agree well with the SFG experimental result. This research demonstrates the feasibility and power of using isotope labeling SFG to probe molecular structures of interfacial biological molecules in situ in real time.

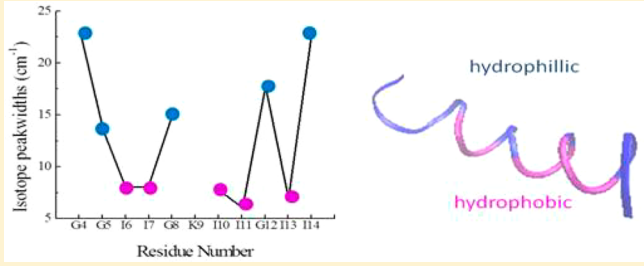

INTRODUCTION

Interfacial properties and functions of peptides and proteins are determined by their molecular structures. Therefore, it is important to obtain structural information on peptides and proteins at interfaces, especially in biomolecule-relevant research fields such as enzyme engineering, drug delivery and membrane chemistry/biology.[1−3]

Vibrational spectroscopic studies on isotope labeled samples have been successfully used to obtain site-specific structural knowledge on peptides and proteins. Because peak frequency and line width are indicators for protein secondary structure and backbone solvation, the amide I band, which mainly consists of the C═O stretching mode contributions, is often analyzed in vibrational spectroscopy. Isotope labeling the $^{12}C{=}^{16}O$ group into $^{13}C{=}^{16}O$ or $^{13}C{=}^{18}O$ isolates an amide I oscillator by introducing a frequency shift of ∼40 cm^{-1} or ∼66 cm^{-1}, respectively.[4] One-dimensional infrared spectroscopy has utilized the amide I peak-centers of the isotope labeled segments to study a variety of topics: α-helix stability, amyloid formation, and local environmental differences in hydrogen bonding for coiled-coil peptides.[4] Furthermore, two-dimensional infrared spectroscopy (2DIR) can measure both the homogeneous and inhomogeneous line widths of isotope labeled amino acids in the peptides, providing information about backbone disorder and local environment fluctuations.[5−8] By comparing the coupling constants between various isotope labeled vibrational pairs, 2DIR has shed light on the 3D tertiary structure of a transmembrane protein.[9] Besides the information provided by frequency and line width analysis, the signal intensity generated by an isotope labeled unit (we will refer to it as "isotope peak" throughout this article) detected using light with different polarizations can be used to determine the angles of individual amino acid dipole moments relative to the surface normal of a stacked bilayer in a FTIR cell.[10] Besides isotope labeled segments, other IR probes such as nitrile, azide and thiocynate functionalities have been incorporated into membrane proteins to acquire site-specific structural and dynamic information.[11−16]

Sum Frequency Generation (SFG) vibrational spectroscopy is a vibrational spectroscopic technique based on second-order nonlinear optical processes.[17−21] It measures the second-order nonlinear optical susceptibility $\chi^{(2)}$, which is nonzero only when the inversion symmetry of the sample is broken (under the electric dipole approximation). This makes SFG an intrinsically

Received: April 18, 2015
Published: August 4, 2015

DOI: 10.1021/jacs.5b04024
J. Am. Chem. Soc. 2015, 137, 10190−10198

surface-sensitive technique which excludes the signal contributions from the sample bulk. During the past decade, SFG has been used to investigate the conformation and orientation of peptides and proteins at interfaces.[22−28] More recently, by deuterium isotope labeling the side chains of a model peptide LKα14 and calculating individual side chain orientations, researchers have shown that SFG has the potential to perform structural determination of biomolecules at an interface, such as on an inorganic surface, which is difficult to study using traditional techniques such as X-ray diffraction or NMR spectroscopy.[29,30]

Previously we have successfully demonstrated the feasibility of detecting SFG signals from a single isotope-labeled backbone $^{13}C{=}O$ unit in the α-helical region of peptide ovispirin-1 (Figure 1) at a polystyrene/peptide solution interface. We

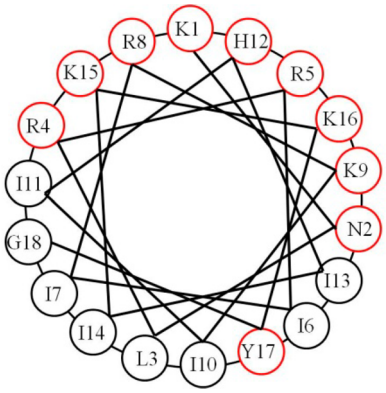

Figure 1. Helical wheel diagram of ovispirin-1. The polar amino acids are circled in red while the nonpolar ones in black.

showed that the detection of the isotope peak allows us to deduce the orientation of a single amide I unit.[31] In this current study, we focused on a more biologically relevant system than the polystyrene surface: ovispirin-1 associated with a lipid bilayer serving as a model cell membrane. To the best of our knowledge, this is the first time to demonstrate experimentally that the SFG line width and peak-center frequency of vibrational probes ($^{13}C{=}O$ in our case) are indicators of peptide local environment. Previously, solid-state NMR results showed that ovispirin-1 lies primarily in the plane of the mixed palmitoyl-2-oleoyl-*sn*-glycero-3-phosphocholine: 1-hexadecanoyl-2-(9Z-octadecenoyl)-*sn*-glycero-3-phospho-(1′-rac-glycerol) (sodium salt) (hereafter referred to as POPC:POPG) bilayer with a tilt angle of ∼84 degrees relative to the surface normal.[32] 2DIR, combined with molecular dynamics simulation, similarly suggested that the α-helical structure and planar orientation of ovispirin-1 associated with mixed POPC:POPG vesicles. The trend in the 2DIR line widths of different isotope labeled residues in the peptide provided additional information to show that the hydrophilic residues of ovisprin-1 were facing the lipid headgroups.[6] Here we used ten different ovispirin-1 mutants, each isotope labeled at a specific site in the α-helical region of the peptide. We investigated the variations of the SFG signal generated from these mutants, including line width, peak frequency and intensity as a function of the residue number. We found that the variance trend in the SFG peak line width and frequency originating from the isotope labeled amino acid residues indicated that ovispirin-1 is lying beneath the headgroups of the 1,2-dipalmitoyl-*sn*-glycero-3-phospho-(1′-*rac*-glycerol) (sodium salt) (hereafter referred to as DPPG) bilayer. Additionally, the positive/constructive interference of all the isotope peaks with the main peak contributed by the unlabeled components suggests that the peptide tilts more toward the surface normal in the DPPG bilayer than in the POPC:POPG = 3:1 vesicles previously reported.[6]

We believe that applying isotope labeled SFG to study biological molecules is innovative and unique. First, SFG has intrinsic surface/interface specificity. Therefore, it is convenient to study biological molecules such as peptides and proteins at many different interfaces, including abiotic/biotic interfaces as well as cell membranes using SFG. Many different vibrational spectroscopic techniques have been used to study proteins and peptides at various interfaces, but the signals of surface/interfacial biomolecules may be easily convoluted by signals contributed from bulk media (e.g., from both solvents and solutes), since these techniques are not intrinsically surface-sensitive. Second, the vibrational spectroscopic probe (e.g., IR probe) functionality may generate signals overlapping/interfering with other signals generated from the molecules on the surface/interface in various vibrational spectroscopic techniques. Isotope labeling breaks local symmetry and can enhance SFG signal because the SFG signal can only be generated from functional groups with no inversion symmetry. This approach can also greatly minimize the possible signal overlapping/interfering with other groups because very likely such groups possess inversion symmetry. For instance, the absorbance of peptide side-chains (e.g., The NH_2 bending mode of Asn or Gln at ∼1580−1625 cm^{-1} and the COO^- asymmetric stretching mode of Asp or Glu at ∼1550−1590 cm^{-1}) can be a concern in isotope labeled IR spectroscopy due to the overlap with isotope labeled amide I peaks.[33] However, this is less of a problem in SFG. The SFG optical response is from an ensemble of all the molecules and different directions of the side chain groups will result in partial or total signal canceling of SFG signal. That is to say, some probes that are not suitable in linear or multidimensional IR studies can be adopted in SFG to study site-specific structures and dynamics.

EXPERIMENTAL SECTION

Materials. Regular ovispirin-1 (with the sequence H_2N-KNLRR IIRKI IHIIK KYGCOOH) and isotope labeled samples were synthesized by Peptide 2.0 Inc. The $^{12}C{=}O$ groups of I6, I7, I10, I11, I13 and I14 were isotope labeled into $^{13}C{=}O$ groups. The R4, R5, R8, H12 residues were mutated into $^{13}C{=}O$ isotope labeled G4, G5, G8 and G12 to reduce the synthesis expense. Previously, research with MD simulations has shown that mutation does not change the property and behavior of ovispirin-1 peptides.[6]

SFG Spectroscopy. Details on SFG theory[34−36] and our near-total-reflection SFG experimental geometry[37,38] have been presented in previous publications. In SFG experiments, we overlapped two laser beams (i.e., one visible beam at 532 nm and one frequency tunable infrared beam from 1100 to 4300 cm^{-1}) spatially and temporally at the bottom side of a right-angle CaF_2 prism. The DPPG/dDPPG bilayer was deposited on the CaF_2 prism with Langmuir−Blodgett and Langmuir−Schaefer method for the outer (deuterated DPPG) and inner (DPPG) leaflets, respectively.[38,39] After the deposition, the lipid bilayer was immersed in a 2 mL water reservoir throughout the SFG spectra collection process. The water subphase was changed to 0.2 mM pH = 7.1 buffer before adding ovisipirin-1 peptide. 20 μL ovisipirin-1 stock solution (1.0 mg/mL) was added into the subphase to achieve a final concentration of 10 μg/mL. A magnetic microstirrer was used to facilitate the homogeneous distribution of ovispirin-1 molecules in the subphase in contact with the lipid bilayer. The experiments were carried out under room temperature (∼20 °C) and the DPPG/dDPPG bilayer remained in gel phase. A time dependent

DOI: 10.1021/jacs.5b04024
J. Am. Chem. Soc. 2015, 137, 10190−10198

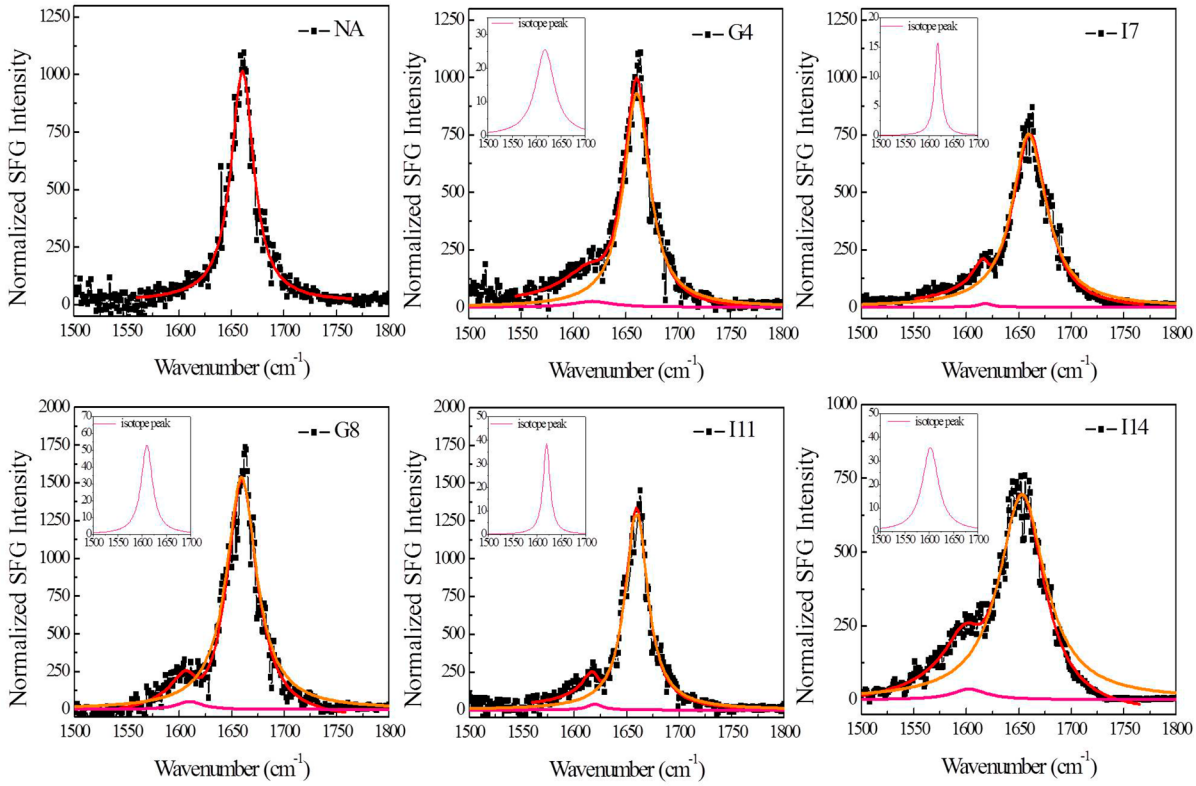

Figure 2. SFG ppp spectra collected from regular ovispirin-1 (NA) and ovispirin-1 isotope labeled at different sites (G4, I7, G8, I11 and I14) in the amide I frequency range when associated with a DPPG/dDPPG bilayer. Orange and magenta lines represent contributions of the main peaks and the isotope labeled peaks, respectively. The fitted isotope labeled peaks are enlarged in the insets.

SFG signal at 1655 cm^{-1} was used to monitor the in situ adsorption of ovispirin-1 to the lipid bilayer as a function of time. SFG spectra in the amide I range were subsequently collected. The optical setup was placed in a nitrogen chamber to minimize the sharp spectra dips in the amide I range resulting from the water vapor absorption of the IR beam in the optical pathway.

The SFG spectrometer is a picosecond frequency scanning system from Altos Inc. The pump laser is a Nd:YAG laser, with an output at 1064 nm, pulse width of 20 ps, and a repetition rate of 20 Hz. The spectral resolution is 4 cm^{-1}, which is sufficient for frequency and line width observation of the isotope labeled peaks. SFG ssp (s-polarized SFG signal beam, s-polarized IR input beam, p-polarized visible input beam) and ppp spectra in the amide I frequency range were collected from ovispirin-1 peptide molecules at the model cell membrane interface using a near total reflection geometry with a step of 1 cm^{-1}. The spectral fitting procedure and peptide orientation analysis are illustrated in detail in the Supporting Information.[37]

Calculation with the Hamiltonian Approach. The parameters in the calculation using the Hamiltonian approach were described in detail previously.[31] The one exciton Hamiltonian is constructed with the amide I vibrational modes of each residue as the local oscillators. The couplings between local modes were calculated by transition-dipole coupling model. The transition dipole was defined to orient 10 degrees[40] while the Raman tensor 34 degrees[41] away from the CO bond of a local mode. The vibrational frequency for an isolated unlabeled oscillator is ~1645 cm^{-1}, which corresponds to a diagonal force constant (DFC) of 1.605 mdyn $Å^{-1}$ cm^{-1}.[42] The frequency for the isotope labeled mode was set to be 1620 cm^{-1}.

MD Simulation Details. The starting structure of the ovispirin-1 was obtained from PDB entry 1HU5[43] and caped with ACE and CT3 at N and C termini, respectively. The protonation of each residue was determined at pH = 7 based on the pK_a of the side chain. The peptide was inserted in two different membrane bilayers, a pure DPPG bilayer with negatively charged head-groups which mimics the bilayer utilized in this study and a mixture of POPC:POPG which is composed of zwitterionic (POPC) and negatively charged POPG lipids with a 3:1 ratio which was previously used by Woys et al.[6] The starting configuration of the peptide inserted in DPPG and POPC:POPG bilayers was constructed by the CHARMM-GUI membrane builder.[44,45] An average of 64 and 62 lipid molecules were accommodated in each leaflet of the DPPG and POPC:POPG bilayers, respectively. TIP3P[46] water models and neutralizing K^+ ions were added to solvate the membranes and peptides. All MD simulations were performed using CHARMM36 force field for lipids[47] and proteins.[48] The equilibration runs were performed following the CHARMM-GUI[44,45] server in NPT ensemble. The production runs were performed using NPγT for DPPG and NPAT for POPC:POPG bilayers to mimic the previous simulations.[6] The surface tension of the bilayer in DPPG simulation was set to 34.0 dyn/cm. The production runs were 100 ns long from which the last 80 ns were used for analysis. Both of the simulations were performed on a GPU platform. The temperatures were kept constant using Andersen heatbath method with coupling constant of 500 ps^{-1}. MC barostat was used to keep the normal pressure constant at 1 atm. The short-range van der Waals interactions were smoothly switched off by a force-switching function at a twin range cutoff between 10 and 12 Å. The long-range electrostatic interactions were calculated using the Particle Mesh Ewald method. The SHAKE algorithm was used to constrain the bond involving hydrogen atoms. The time step was chosen to be 2 fs. The distance of each Cα atom was calculated as distance of each Cα atom from the average positions of the C2 atoms of the leaflet that the peptide was inserted in, along the membrane normal (z axis).

RESULTS AND DISCUSSION

SFG Spectra of Isotope Labeled Ovispirin-1 Samples. After adding the ovispirin-1 peptide stock solution into the subphase in contact with the DPPG/dDPPG bilayer, the SFG amide I signal at 1655 cm^{-1} contributed by the ovispirin-1 α-helical structure increased for 200 s and then remained stable

DOI: 10.1021/jacs.5b04024
J. Am. Chem. Soc. 2015, 137, 10190−10198

Table 1. Fitting Parameters of SFG ppp Spectra Collected from Ovispirin-1 with and without Isotope Labeled Units at Different Sites[a]

	isotope peak-center (cm^{-1})	isotope line width (cm^{-1})	main peak-center (cm^{-1})	main peak line width (cm^{-1})	$\chi_{isotope\ peak}/\chi_{main\ peak}$
NA	NA	NA	1660.5 ± 0.2	13.4 ± 0.4	0
G4	1618.0 ± 0.7	23 ± 1	1659.0 ± 0.9	15.1 ± 0.2	0.20 ± 0.02
G5	1608 ± 2	14 ± 5	1661.8 ± 0.5	13.0 ± 0.1	0.068 ± 0.005
I6	1614.0 ± 0.8	8 ± 1	1662.7 ± 0.1	25.6 ± 0.1	0.059 ± 0.004
I7	1618.0 ± 0.7	8 ± 1	1660.7 ± 0.1	19.8 ± 0.5	0.148 ± 0.006
G8	1610.0 ± 0.2	15 ± 2	1659.3 ± 0.1	16.8 ± 0.6	0.184 ± 0.002
I10	1616.0 ± 0.1	8 ± 1	1657.9 ± 0.3	15.5 ± 0.1	0.135 ± 0.001
I11	1620.0 ± 0.4	6 ± 2	1659.3 ± 1.0	12.8 ± 0.9	0.16 ± 0.01
G12	1607 ± 1	18 ± 2	1658.7 ± 0.4	16.3 ± 0.1	0.18 ± 0.01
I13	1616 ± 1.2	7 ± 1	1659.7 ± 0.6	14.4 ± 0.1	0.13 ± 0.01
I14	1606 ± 3	23 ± 2	1655.6 ± 1.3	23.0 ± 2.0	0.21 ± 0.03

[a]The error bars are standard deviations from four measurements of two independent experiments.

for the next few hours (for the full duration of our SFG experiments). SFG spectra collected in the C−H and C−D stretching frequency ranges, which are generated by the lipid chains of the hydrogenated inner leaflet and deuterated outer leaflet, respectively, were collected before adding peptide to the subphase and after the 1655 cm^{-1} signal became stable. Since ovispirin-1 is an antimicrobial peptide, above a certain solution concentration, it can disrupt the model cell membrane (lipid bilayer) severely. In that case, the peptide molecules are likely to adopt multiple orientations,[26,49] making our site-specific observations on isotope labeled peptides difficult to interpret. In that situation, the bilayer leaflets would undergo fast flip-flop and result in the decrease of SFG signals detected from each leaflet. However, this is not the case here. In this study, for both lipid leaflets, the SFG C−H and C−D stretching spectra have minimal changes (Figure S1 in Supporting Information), which suggested that during the peptide-lipid bilayer interaction process, the lipid bilayer does not have large structural changes such as the formation of toroidal pores[50] or the fast flip-flop.[51] We have shown previously that, when the peptide solution concentration was low, the peptides more likely adopt a relatively uniform orientation, different from the case where the peptides disrupt the lipid bilayer.[26,49] The peptide uniform orientation provides a good case for this isotope labeled peptide study.

SFG spectra in the amide I range were collected from ten isotope-labeled ovispirin-1 mutants as well as the nonisotope-labeled ovispirin sample associated with the DPPG/dDPPG lipid bilayer. In Figure 2, we present five typical SFG spectra (all in ppp polarization as some isotope peaks cannot be resolved in the ssp spectra) detected in the amide I frequency range and the rest five SFG spectra are shown in the Supporting Information Figure S2. For all the peptide samples, the amide I peaks are centered at ∼1660 cm^{-1} which agrees with the typical peak-center for α-helices.[52] The isotope peak appears as a shoulder of the main peak. The isotope peak-center varies from 1606 to 1620 cm^{-1} and the line width spans from 6 to 24 cm^{-1} with isotope labels at different amino acid positions. Note that the isotope labeled peaks are amplified due to the interference with the main peak, which is the reason that the shoulders (red line in Figure 2) appear larger than the individual isotope labeled contributions (pink line in Figure 2). Previously researchers have shown that using interference effects, weak SFG signal at an interface could be detected by choosing appropriate substrate thickness.[53] Here, we demonstrate that signals for vibrational SFG probes can be enhanced using interference effects. Besides, the intensity of the isotope peak changes with different isotope labeling sites. In order to quantify this effect, we fit the SFG amide I spectra with two peaks and calculated the $\chi_{isotope\ peak}/\chi_{main\ peak}$ ratio. The fitting parameters for these SFG spectra are summarized in Table 1. Next we will explain what the peak-center, line width and $\chi_{isotope\ peak}/\chi_{main\ peak}$ ratio variations imply in terms of peptide location, structural disorder and site-specific orientation.

Implications of the Isotope Peak-centers and Line widths. Previous 2DIR line width studies have indicated that the homogeneous line width of a specific isotope labeled residue is an intrinsic property of the peptide and the inhomogeneous broadening is a probe of the structure disorder (measured by hydrogen-bond length) and the environment (measured by electrostatic interactions) around that residue.[6,8] Similarly, FTIR, which measures the total line width, can also be used to probe the different environments of various peptide amino acid residues. Recently, the total line width information was extracted from FTIR spectra to map the environmental polarity in proteins.[54] Here, as shown in Figure 3a, SFG isotope peaks of the amino acids that are on the hydrophilic face of the α-helix, G4, G5, G8 and G12 have wider line widths than those of the residues on the hydrophobic face, I6, I7, I10 and I11. It was shown previously that the region from G4 to I16 in ovispirin-1 forms well-defined α-helical structure[6,43] associated with lipids or lipid-mimic agent TFE and thus the differences of the line widths in Figure 3a are mainly due to electrostatic interactions rather than structural disorder. This line width variation trend agrees with the previous 2D-IR diagonal line width (total and inhomogeneous line width) study and indicates that the peptide is buried beneath the lipid headgroups. Large line width variation of the isotope peaks contributed by the G4 (23 cm^{-1}), G5 (14 cm^{-1}), G8 (15 cm^{-1}) and G12 (18 cm^{-1}) amino acid residues are induced by the lipid headgroups and water while smaller line width variation for I6 (8 cm^{-1}), I7 (8 cm^{-1}), I10 (8 cm^{-1}) and I11 (6 cm^{-1}) are caused by the hydrophobic lipid interior.[6,54] Our study here has successfully demonstrated that the total line widths of SFG isotope peaks can be used as a sensitive environmental probe for membrane-associated peptides. However, cautions need to be taken when extending this method to systems where the invariability of the homogeneous line widths is undetermined. For membrane peptides, this is shown to be a good assumption.[6,55] If variability in the homogeneous line width is suspected, it can be double checked using 2D IR or 2D SFG spectroscopy.[56]

DOI: 10.1021/jacs.5b04024
J. Am. Chem. Soc. 2015, 137, 10190−10198

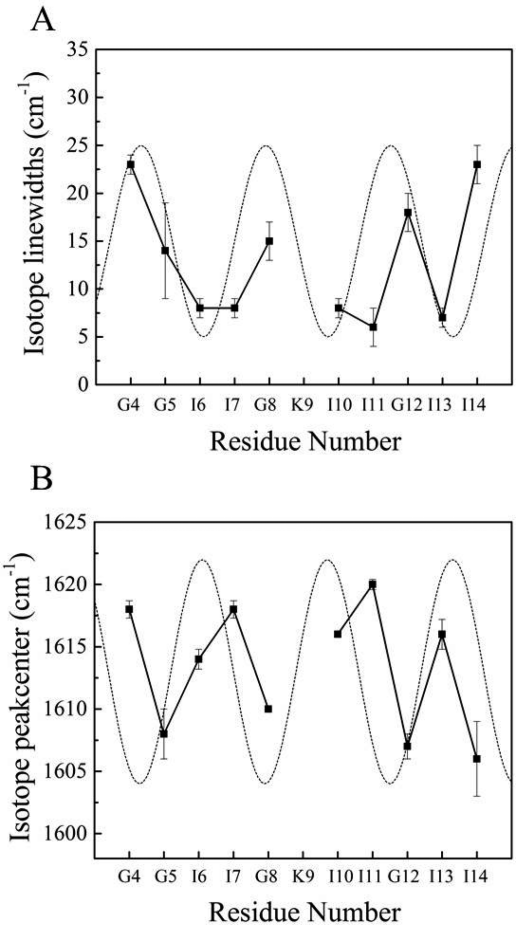

Figure 3. (A) Line widths and (B) peak-center frequencies of the collected SFG isotope peaks as a function of isotope labeled amino acid residue number. The sinusoidal lines show the periodical structure of an ideal α-helix.

The line width of the SFG signal detected from I14 is very different from what was measured by 2DIR.[6] I14 is on the hydrophobic face of the peptide helical wheel and exhibited a narrow diagonal line width in the 2DIR study of ~12 cm^{-1}.[6] However, in SFG measurement, the line width was ~24 cm^{-1}. It is worth noting that in the 2DIR experiment, ovispirin-1 was studied when associated with a mixed POPC:POPG bilayer, while SFG experiments were carried out on a DPPG bilayer. In the aforementioned 2DIR experiments, signals detected from the isotope labeled peaks of K15 and K16 had an abrupt increase in line width which was attributed to the denaturation of the peptide starting from those two amino acids. Here, likely due to the large negative-charge density of DPPG, the peptide denaturation starts earlier at residue I14 and the larger line width of the SFG signals detected form I14 is an indicator of structural disorder.

Figure 3b displays the peak-center frequencies of different isotope labeled peaks, which have a similar sinusoidal variation trend compared to the line width. The isotope peak-center frequencies for G5, G8 and G12 are lower, while the peak-center frequencies of the signals detected from I6, I7, I10 and I11 are higher. This indicates that inside the core α-helical structure, the peak-center frequency of the isotope labeled $^{13}C{=}O$ group is a probe to the local electrostatic interaction. As indicated above, the G5, G8 and G12 are interacting with lipid head groups, while I6, I7, I10 and I11 are facing the hydrophobic lipid interior.

However, although G4 has a wide line width, similar to that of G5, G8 and G12, its peak-center remains at a higher frequency, different from the other residues. The fact that both the SFG signal peak-centers from G4 and I14 have the highest frequencies suggests that the sinusoidal trend breaks down at the ends where the α-helix unravels. This agrees with the results obtained from the previous 2DIR study where the frequency is correlated with the hydrogen-bond length.[8] While the line width reflects the dynamics of hydrogen-bond length and electric fields, peak-center frequency prediction requires knowing both the absolute hydrogen-bond length and electric fields. Therefore, their variation trends are correlated but not the same.

The Intensities of the Isotope Peaks Are Related to Peptide Orientation. The intensity of an SFG signal detected from a chemical group is sensitive to the orientation of that chemical group.[57] In order to gain some insight into the isotope labeled carbonyl group orientation, we fitted the spectra with two peaks (Table 1), observed a sinusoidal variation trend of χ_{label}/χ_{main} ratio (Figure 4), and found that all the isotope peaks

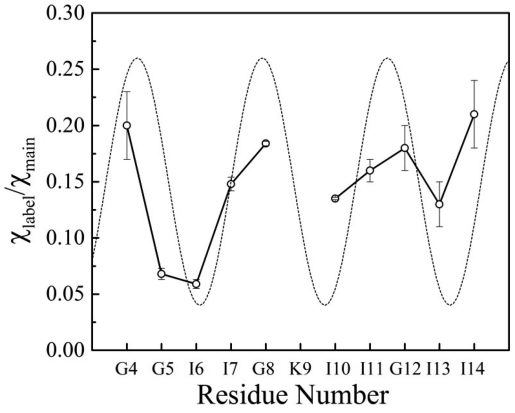

Figure 4. Experimentally measured SFG signal strength ratio χ_{label}/χ_{main} as a function of residue number.

have positive interferences with the main peak. Previously, SFG spectra from different polarization combinations have been utilized to deduce orientations of different secondary structures such as α-helices,[41,58] 3_{10} helices[41,59] and β-sheets.[60,61] Such studies require knowledge of the amide I mode molecular hyperpolizabilities for those secondary structures. To calculate the hyperpolarizability, a perturbation treatment which has been used to calculate IR response for infinite regular polypeptide chains was adopted.[62] In this treatment, signal amplitudes of peptide SFG-active groups (e.g., the A mode and E1 mode for the α helix) were calculated from the symmetry relations between local modes generated by individual amino acid residues. In this current study, because an isotope label was incorporated into different sites of an α-helix, the symmetry of the local modes was severely disrupted. Thus, we adopt the Hamiltonian approach to solve the eigenvalue problem for the Hamiltonian matrix. In other words, the labeled local mode will disrupt the symmetry so that the spectrum will change from two dominated exciton modes (namely A mode and E1 mode) to more complicated lineshapes. In order to understand what the sinusoidal variation trend of χ_{label}/χ_{main} ratio implies we simulated SFG spectra corresponding to an ideal helix (with

DOI: 10.1021/jacs.5b04024
J. Am. Chem. Soc. 2015, 137, 10190−10198

one amino acid isotope labeled at a different site) that tilted at different angles from the surface normal using the Hamiltonian approach (Supporting Information Figure S3). For an ideal helix, when the tilt angle of the helix axis is 0 degree relative to the surface normal (i.e., standing up on the surface), all the amide I transition dipoles have the same orientation relative to the surface normal and the χ_{label}/χ_{main} ratios are the same for samples with different residue isotope labeled. However, when the peptide has a tilt angle of 60 degrees, the z projection of the amide I modes has a sinusoidal variation as a function of the residue number that matches the χ_{label}/χ_{main} ratio with a 3.6 residue pitch. When the peptide has an even bigger tilt angle such as 80 degrees, some of the isotope peaks start to have a different phase from the main peak (destructive interference occurs). This is because while the helical axis is 80 degrees relative to the surface normal which still points toward the positive direction of the z axis (i.e., pointing up), some peptide segment amide I transition dipoles point to the negative direction of the z axis (i.e., pointing down). Due to the different absolute orientations, SFG signals exhibit different phases. Previously, researchers have shown that from the SFG spectral interference between the methyl groups on the octadecyltrichlorosilane (OTS) monolayer substrate and those on Trimethylamine *N*-Oxide (TMAO) molecules,[63] the absolute orientation of the methyl groups on TMAO could be deduced. Here we have shown that this approach can be used for isotope labeled amino acids as well.

Our results have shown that all the isotope peaks have positive interference with the main peak and therefore all the amide I transition dipoles of amino acid segments at different positions have the same absolute orientation. The comparison between the experimental and simulated data suggests that different from the POPC:POPG = 3:1 case where the peptide almost lies flat in the membrane, the peptide axis has a smaller tilt angle θ_2 relative to the surface normal when associated with a DPPG lipid bilayer (Figure 5). The angle θ_3 between the principal axis of the amide I mode of a peptide unit and the principal axis of the helix is ~24° in our calculation and thus the upper limit of θ_2 is 66° (90° − θ_3). For θ_2 > 66°, the amide I mode of a peptide unit can point to a negative direction,

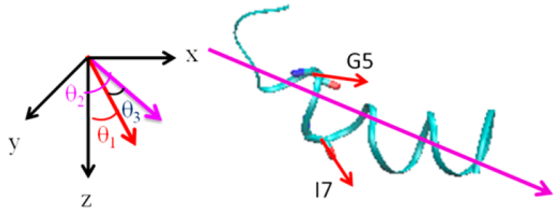

Figure 5. Schematic showing possible orientation of ovispirin-1 backbone and individual residues. The z axis positive direction is pointing to the lipid hydrophobic core region. θ_1 is the acute angle between the transition dipole of the $^{13}C{=}O$ chemical group (opposite direction of the red arrow) and the z axis, and θ_2 is the acute angle between the peptide helix axis (from N to C terminus) (purple arrow) and the z axis. θ_3 is the acute angle between the transition dipole of $^{13}C{=}O$ chemical group and the peptide helix axis, which is ~24° in our calculation. From the experimental results, all transition dipoles are pointing to the same direction and thus the boundary condition corresponding to the transition dipole moment of hydrophilic residues such as G5 are parallel to the xy plane leading to a $\theta_2 = 90° - \theta_3$. The transition dipoles of the $^{13}C{=}O$ chemical groups in I7 and I11 are calculated to be 38° relative to z axis (see details in the next section).

leading to negative interference with the main peak, which was not observed. Therefore, we believe $\theta_2 \leq 66°$. We have simulated the ratios of χ_{label}/χ_{main} for isotope labeled residues as a function of the peptide tilt angle and the results are presented in the Supporting Information.

Site-Specific Orientation of I7 and I11. Previously we showed that the χ_{zzz}/χ_{xxz} ratio of a single amide I unit can be derived from the SFG isotope peak taken with different polarization combinations: ssp and ppp.[31] By correlating the experimentally measured χ_{zzz}/χ_{xxz} ratio with the theoretical tilt-angle dependence curve, the tilt angle θ of the isotope labeled transition dipole relative to the membrane surface normal can be deduced. In this work, we successfully obtained quantitative fitting parameters from the isotope peak in the ssp spectra for two isotope labeled peptides: I7 and I11. The tilt-angle dependences of χ_{zzz}/χ_{xxz} for Ψ-averaged, Ψ = 0°, and Ψ = 90° cases, where Ψ is the rotational angle around the isotope labeled transition dipole, were reported.[31] There is less than a 10° difference for the calculated tilt angles between the Ψ-averaged and the Ψ-fixed (0 or 90°) cases and thus here we only show the result for the Ψ-averaged cases (Table 2),

Table 2. SFG Susceptibility Ratio χ_{zzz}/χ_{xxz} Derived from the Fitting Results of the Isotope Peaks in the ppp and ssp SFG Spectra Collected from I7 and I11[a]

	χ_{zzz}/χ_{xxz}	θ_δ/°	$\theta_{Gaussian}$/°
I7	2.30 ± 0.20	38 ± 3	38 ± 3
I11	2.28 ± 0.08	38 ± 2	38 ± 2

[a] θ_δ and $\theta_{Gaussian}$ are deduced tilt angles of amide I transition dipole moment relative to the surface normal, assuming a δ distribution and Gaussian distribution with 15 degrees of full-width-at-half-maxima, respectively, in a Ψ-averaged case (Ψ is the rotational angle around the isotope labeled transition dipole). The error bars are standard deviations from four measurements of two independent experiments.

assuming a δ distribution and Gaussian distribution with 15 degrees of full-width-at-half-maximum (fwhm) for the tile angle θ. The choice for the 15 degrees of fwhm is arbitrary, which enable us to observe how much structural heterogeneity would affect the result. Taking together the experimental error bars (±2° and ±3°) reported in Table 2 and the error bars introduced by using Ψ-averaged curve (±10°), the tilt angles of amide I transition dipole moment relative to the surface normal for residue 7 and 11 are 38 ± 10°. Here the calculated angle is very close to the reported magic angle 39.2° which includes the possibilities that the tabulated chemical groups are randomly oriented at the interface.[64] However, our isotope peak line widths data support that the ovispirin-1 peptide is sandwiched in the lipid bilayer and the helical backbone has limited rotational freedom and narrow orientation distribution. Besides, MD simulation data suggest that the orientation distributions of the residues 7 and 11 can be fitted with Gaussian functions with 9.4 and 10.4 degrees of fwhm, respectively (Supporting Information). Taking together, we believe our assumption of "narrow orientation distribution" is reasonable. We need to emphasize that the method used here cannot distinguish the difference between a transition dipole pointing to the positive z axis (θ) and the negative z axis (180-θ) with the same tilt angle. For instance, the θ_δ for I7 was determined to be either 38 ± 10° or 142 ± 10°. With the advent of phase-sensitive SFG,[65−67] it is possible to deduce the absolute orientation of vibrational probes without interference effect in the future. Since both I7

DOI: 10.1021/jacs.5b04024
J. Am. Chem. Soc. 2015, 137, 10190−10198

and I11 are on the hydrophobic side of the peptide, and we have mentioned above the angle θ_3 between the principal axis of the amide I mode of a peptide unit and the principal axis of the helix is ~24 degrees in our calculation, we can deduce that the helical axis tilted less than 62° (38°+ θ_3) relative to the surface normal which agrees with the conclusion obtained in the previous section (Figure 5).

MD Simulation Results. In order to understand the discrepancy of the peptide orientations in the two bilayer systems, namely, a highly negative DPPG bilayer in our study and a moderately negative mixture of POPC:POPG = 3:1 bilayer reported by Woys et. al,[6] here, we have looked at the insertion profile of different amino acids of the peptide by performing MD simulation. As depicted in Figure 6, in both

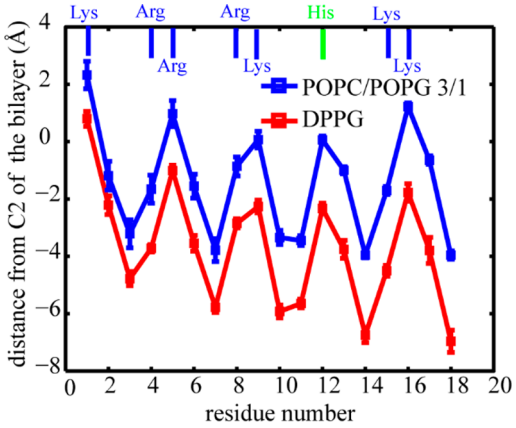

Figure 6. Distance from the membrane surface for backbone Cα of each residue. The results from a simulation of the peptide in a POPC/POPG bilayer are in blue while those in a DPPG bilayer are shown in red. The positions of the charged residues (i.e., Lys and Arg) in the sequence of the peptide are marked with blue bars on top of the figure. The position of His residue is indicated with a green bar since the His residue is considered to be neutral in these simulations.

DPPG and POPC:POPG bilayers, the N terminal helix (residues 1−10) inserts slightly less and is located closer to the headgroup region compared to the C terminus (residues 11−18). This difference can be related to the charge distribution in the sequence of the peptide. In the N terminus of the peptide, five positively charged side chains can have favorable interactions with the negatively charged headgroup atoms. On the other hand, the C terminus of the peptide only contains two positive side chains and higher number of long and hydrophobic residues which makes insertion into the hydrophobic lipid bilayer core slightly more favorable. Our results suggest that the interactions between the hydrophobic side chains and the lipid tails are weighed slightly heavier in the C terminal region of the peptide. The difference between the peptide insertion profiles in the DPPG and POPC/POPG = 3:1 bilayers can be attributed to the different compositions of the two lipid bilayers and their different responses to the presence of a charged peptide side chain. As discussed above, the more tilted peptide orientation has been observed with the positive interferences in SFG signals, matching the simulation data. It is worth mentioning that the time span of 100 ns that is used in our simulations is not long enough to allow for multiple association and dissociation events of the peptide and the membranes to occur and therefore the position of the peptide may be affected by the initial configurations in each of the membranes. In addition, the protonation states of the charged side chains are fixed based on their reference pK_a. However, insertion into the lipid bilayer and interaction with lipid headgroups can alter the pK_a values and the charge.[68] This is particularly true for His12 and the same logic applies to the N and C terminals of the peptide. While both N and C terminals are caped with appropriate patches (namely, N-terminal acetylation and C-terminal amidation) and left neutral, in the experimental study the terminals are not patched and therefore can adopt different charge states based on their distance from the head groups and other charged residues which may affect the orientation of the peptide. Recently, researchers have reported a computational approach to obtain peptide amide I line width and orientation by combining line-shape theory with MD simulations.[40] Site-specific side-chain computational simulations have also been reported recently.[69] We hope our results will inspire new computational efforts in obtaining peptide site-specific information in the amide I region.

Antimicrobial Behavior of Ovispirin-1. In this work, we found that the ovispirin-1 molecule is located at the interface beneath the bilayer headgroups region in the DPPG lipid bilayer according to the line widths as well as peak-center frequencies in the isotope-labeled SFG spectra. This agrees with previous NMR and 2DIR results. However, our research shows that the peptide adopts a slightly tilted orientation which has not been suggested by previous research. This is likely because the charge density of the model cell membrane has increased from the POPC:POPG = 3:1 system (in previous 2DIR study) to the current pure DPPG system. The key question for studies on antimicrobial peptides is to understand their selectivity toward microbial versus mammalian cells. Our work shown here suggests that it is possible to distinguish the subtle peptide orientational and conformational difference when the peptide is interacting with different types of lipid bilayers using isotope-labeled SFG.

Further Discussion. In this paper, we have reported that $^{13}C{=}O$ can be used as an SFG vibrational probe for studying site-specific structural information on peptides associated with a model cell membrane. Recently, a review paper on IR probes has summarized the criteria for useful IR probes[14] and one important requirement is that the probe should have large transition dipole strength for detection. It is more challenging to look for SFG probes in this regard; the second-order nonlinear susceptibility $\chi^{(2)}$ is a Kronecker product of the oscillator's Raman tensor and the transition dipole moment, thus in order for the SFG signal of the probe to be detected, the vibrational mode of the probe needs to be both Raman and IR active. On the other hand this can be beneficial since a weak IR probe may be an applicable SFG probe if the vibrational mode has a large Raman polarizability. Our work presented here has shown that with homodyne detection SFG, the isotope labeled $^{13}C{=}O$ signal can be detected and the peak-center frequency, line width and intensity can be quantified in SFG spectra for peptides associated with model cell membranes. In addition, the intrinsic SFG principle overcomes two limitations of isotope labeling infrared spectroscopy mentioned in the above review:[14] 1. The spectral window of the isotope labeled amide I vibrations overlaps with the infrared band of peptide side chains and this causes a problem in the case of large proteins. For SFG, the contribution from side chains is minimized because, in large-size polypeptides or proteins, side chains are likely point in different directions, which leads to the reduction/cancellation of their SFG signals. 2. The broad combination

DOI: 10.1021/jacs.5b04024
J. Am. Chem. Soc. 2015, 137, 10190−10198

band (2000−2500 cm^{-1}) and water bending mode (~1500 cm^{-1}) brings significant water background contribution in infrared spectroscopy. In SFG, the Raman-inactive water signal is extremely weak and can be ignored. More importantly, isotope-labeled SFG can elucidate site-specific orientation information for biomolecules specifically on a surface or at an interface.[40] This technique can also be applied to larger proteins with the synthesis methods developed recently such as expressed protein ligation, native chemical ligation and expanded genetic code method.[70,71] With the advances in heterodyne detection SFG,[65,72,73] the SFG signal-to-noise ratio of the isotope peaks will be improved and more accurate orientation information can be extracted from SFG signals measured using more polarization combinations such as spp and sps. With the phase information obtained, the absolute (pointing-up or point-down) orientation for site-specific labels can be deduced. The recent advance of two-dimensional SFG[56,74−76] will greatly extend the application of isotope labeling SFG and will provide further insights into peptide/protein dynamics and mode coupling at interfaces.

CONCLUSION

Herein, we studied the interfacial site-specific structure of ovispirin-1 associated with a DPPG lipid bilayer. The sinusoidal trend of SFG line width and peak-center frequency is remarkably similar to that obtained from 2DIR spectroscopy, suggesting the peptide locates at the interface beneath the lipid headgroup region. This indicates that SFG line width and peak-center frequencies can be used as a site-specific environment indicator. The constructive interferences and the sinusoidal trend of the spectral contribution from the isotope labeled $^{13}C{=}O$ chromophores suggests that the peptide was oriented at an upward tilt (the up-limit of the tilt angle is 62−66°) with the N-terminus closer to the headgroup region. With the abundant structural information deduced from isotope-labeled SFG, we believe this method has great potential in the future in peptide and protein interfacial structural determination.

ASSOCIATED CONTENT

Supporting Information

The Supporting Information is available free of charge on the ACS Publications website at DOI: 10.1021/jacs.5b04024.

Experimental SFG spectra of the lipid bilayer and isotope labeled peptides as well as simulated SFG spectra. (PDF)

AUTHOR INFORMATION

Corresponding Authors

*zanni@chem.wisc.edu

*zhanc@umich.edu

Notes

The authors declare no competing financial interest.

ACKNOWLEDGMENTS

This work is supported by the National Institute of Health (1R01GM081655 to ZC and 1R01DK79895 to MTZ). B.D. acknowledges the Rackham Student Research Grant. We thank Dr. Pei Yang for technical support on the SFG spectrometer. We thank Dr. Zunliang Wang for early work and discussions on the MD simulation. We also appreciate Dr. Jeanne Hankett for editing the manuscript.

REFERENCES

(1) Bloom, J. D.; Meyer, M. M.; Meinhold, P.; Otey, C. R.; MacMillan, D.; Arnold, F. H. *Curr. Opin. Struct. Biol.* **2005**, *15*, 447−452.

(2) Petitpas, I.; Bhattacharya, A. A.; Twine, S.; East, M.; Curry, S. *J. Biol. Chem.* **2001**, *276*, 22804−22809.

(3) Opella, S. J.; Marassi, F. M. *Chem. Rev.* **2004**, *104*, 3587−3606.

(4) Decatur, S. M. *Acc. Chem. Res.* **2006**, *39*, 169−175.

(5) Ganim, Z.; Chung, H. S.; Smith, A. W.; Deflores, L. P.; Jones, K. C.; Tokmakoff, A. *Acc. Chem. Res.* **2008**, *41*, 432−441.

(6) Woys, A. M.; Lin, Y.-S.; Reddy, A. S.; Xiong, W.; Pablo, J. J. de; Skinner, J. L.; Zanni, M. T. *J. Am. Chem. Soc.* **2010**, *132*, 2832−2838.

(7) Lin, Y.-S.; Shorb, J. M.; Mukherjee, P.; Zanni, M. T.; Skinner, J. L. *J. Phys. Chem. B* **2009**, *113*, 592−602.

(8) Mukherjee, P.; Kass, I.; Arkin, I. T.; Zanni, M. T. *J. Phys. Chem. B* **2006**, *110*, 24740−24749.

(9) Remorino, A.; Hochstrasser, R. M. *Acc. Chem. Res.* **2012**, *45*, 1896−1905.

(10) Arkin, I. T. *Curr. Opin. Chem. Biol.* **2006**, *10*, 394−401.

(11) Waegele, M. M.; Culik, R. M.; Gai, F. *J. Phys. Chem. Lett.* **2011**, *2*, 2598−2609.

(12) Boxer, S. G. *J. Phys. Chem. B* **2009**, *113*, 2972−2983.

(13) Alfieri, K. N.; Vienneau, A. R.; Londergan, C. H. *Biochemistry* **2011**, *50*, 11097−11108.

(14) Kim, H.; Cho, M. *Chem. Rev.* **2013**, *113*, 5817−5847.

(15) King, J. T.; Arthur, E. J.; Brooks, C. L.; Kubarych, K. J. *J. Phys. Chem. B* **2012**, *116*, 5604−5611.

(16) Thielges, M. C.; Axup, J. Y.; Wong, D.; Lee, H. S.; Chung, J. K.; Schultz, P. G.; Fayer, M. D. *J. Phys. Chem. B* **2011**, *115*, 11294−11304.

(17) Chen, Z.; Shen, Y. R.; Somorjai, G. A. *Annu. Rev. Phys. Chem.* **2002**, *53*, 437−465.

(18) Eisenthal, K. B. *Chem. Rev.* **1996**, *96*, 1343−1360.

(19) Richmond, G. L. *Chem. Rev.* **2002**, *102*, 2693−2724.

(20) Walker, D. S.; Hore, D. K.; Richmond, G. L. *J. Phys. Chem. B* **2006**, *110*, 20451−20459.

(21) Shultz, M. J.; Schnitzer, C.; Simonelli, D.; Baldelli, S. *Int. Rev. Phys. Chem.* **2000**, *19*, 123−153.

(22) Jung, S.-Y.; Lim, S.-M.; Albertorio, F.; Kim, G.; Gurau, M. C.; Yang, R. D.; Holden, M. A.; Cremer, P. S. *J. Am. Chem. Soc.* **2003**, *125*, 12782−12786.

(23) Mermut, O.; Phillips, D. C.; York, R. L.; McCrea, K. R.; Ward, R. S.; Somorjai, G. A. *J. Am. Chem. Soc.* **2006**, *128*, 3598−3607.

(24) Boughton, A. P.; Yang, P.; Tesmer, V. M.; Ding, B.; Tesmer, J. J. G.; Chen, Z. *Proc. Natl. Acad. Sci. U. S. A.* **2011**, *108*, E667−E673.

(25) Fu, L.; Liu, J.; Yan, E. C. Y. *J. Am. Chem. Soc.* **2011**, *133*, 8094−8097.

(26) Ding, B.; Chen, Z. *J. Phys. Chem. B* **2012**, *116*, 2545−2552.

(27) Roeters, S. J.; Dijk, C. N.; Torres-Knoop, A.; Backus, E. H. G.; Campen, R. K.; Bonn, M.; Woutersen, S. *J. Phys. Chem. A* **2013**, *117*, 6311−6322.

(28) Ding, B.; Glukhova, A.; Sobczyk-Kojiro, K.; Mosberg, H. I.; Tesmer, J. J. G.; Chen, Z. *Langmuir* **2014**, *30*, 823−831.

(29) Weidner, T.; Castner, D. G. *Phys. Chem. Chem. Phys.* **2013**, *15*, 12516−12524.

(30) Weidner, T.; Breen, N. F.; Li, K.; Drobny, G. P.; Castner, D. G. *Proc. Natl. Acad. Sci. U. S. A.* **2010**, *107*, 13288−13293.

(31) Ding, B.; Laaser, J. E.; Liu, Y.; Wang, P.; Zanni, M. T.; Chen, Z. *J. Phys. Chem. B* **2013**, *117*, 14625−14634.

(32) Yamaguchi, S.; Huster, D.; Waring, A.; Lehrer, R. I.; Kearney, W.; Tack, B. F.; Hong, M. *Biophys. J.* **2001**, *81*, 2203−2214.

(33) Hamm, P.; Zanni, M. T. *Concepts and Methods of 2D Infrared Spectroscopy*; Cambridge University Press: Cambridge, 2011.

(34) Moad, A. J.; Simpson, G. J. *J. Phys. Chem. B* **2004**, *108*, 3548−3562.

(35) Wang, H.; Gan, W.; Lu, R.; Rao, Y.; Wu, B. *Int. Rev. Phys. Chem.* **2005**, *24*, 191−256.

(36) Lambert, A. G.; Davies, P. B.; Neivandt, D. J. *Appl. Spectrosc. Rev.* **2005**, *2*, 103−145.

DOI: 10.1021/jacs.5b04024
J. Am. Chem. Soc. 2015, 137, 10190−10198

(37) Ye, S.; Nguyen, K. T.; Clair, S. V Le; Chen, Z. *J. Struct. Biol.* **2009**, *168*, 61−77.
(38) Nguyen, K. T.; Clair, S. V Le; Ye, S.; Chen, Z. *J. Phys. Chem. B* **2009**, *113*, 12358−12363.
(39) Tamm, L. K.; Mcconnell, H. M. *Biophys. J.* **1985**, *47*, 105−113.
(40) Carr, J. K.; Wang, L.; Roy, S.; Skinner, J. L. *J. Phys. Chem. B* **2015**, *119*, 8969−8983.
(41) Nguyen, K. T.; Clair, S. V Le; Ye, S.; Chen, Z. *J. Phys. Chem. B* **2009**, *113*, 12169−12180.
(42) Torii, H.; Tasumi, M. *J. Chem. Phys.* **1992**, *96*, 3379−3387.
(43) Sawai, M. V.; Waring, A. J.; Kearney, W. R.; McCray, P. B.; Forsyth, W. R.; Lehrer, R. I.; Tack, B. F. *Protein Eng., Des. Sel.* **2002**, *15*, 225−232.
(44) Jo, S.; Kim, T.; Im, W. *PLoS One* **2007**, *2*, E880.
(45) Jo, S.; Lim, J. B.; Klauda, J. B.; Im, W. *Biophys. J.* **2009**, *97*, 50−58.
(46) Jorgensen, W. L.; Chandrasekhar, J.; Madura, J. D.; Impey, R. W.; Klein, M. L. *J. Chem. Phys.* **1983**, *79*, 926−935.
(47) Klauda, J. B.; Venable, R. M.; Freites, J. A.; Connor, J. W. O.; Tobias, D. J.; Mondragon-ramirez, C.; Vorobyov, I.; Mackerell, A. D.; Pastor, R. W. *J. Phys. Chem. B* **2010**, *114*, 7830−7843.
(48) Best, R. B.; Zhu, X.; Shim, J.; Lopes, P. E. M.; Mittal, J.; Feig, M.; Mackerell, A. D. *J. Chem. Theory Comput.* **2012**, *8*, 3257−3273.
(49) Yang, P.; Ramamoorthy, A.; Chen, Z. *Langmuir* **2011**, *27*, 7760−7767.
(50) Chen, X.; Wang, J.; Kristalyn, C. B.; Chen, Z. *Biophys. J.* **2007**, *93*, 866−875.
(51) Liu, J.; Brown, K. L.; Conboy, J. C. *Faraday Discuss.* **2013**, *161*, 45−61.
(52) Tamm, L. K.; Tatulian, S. A. *Q. Rev. Biophys.* **1997**, *30*, 365−429.
(53) Ye, S.; Tong, Y.; Ge, A.; Qiao, L.; Davies, P. B. *Chem. Rec.* **2014**, *14*, 791−805.
(54) Manor, J.; Feldblum, E. S.; Zanni, M. T.; Arkin, I. T. *J. Phys. Chem. Lett.* **2012**, *3*, 939−944.
(55) Manor, J.; Mukherjee, P.; Lin, Y.-S.; Leonov, H.; Skinner, J. L.; Zanni, M. T.; Arkin, I. T. *Structure* **2009**, *17*, 247−254.
(56) Laaser, J. E.; Skoff, D. R.; Ho, J.-J.; Joo, Y.; Serrano, A. L.; Steinkruger, J.; Gopalan, P.; Gellman, S. H.; Zanni, M. T. *J. Am. Chem. Soc.* **2014**, *136*, 956−962.
(57) Zhuang, X.; Miranda, P.; Kim, D.; Shen, Y. *Phys. Rev. B: Condens. Matter Mater. Phys.* **1999**, *59*, 12632−12640.
(58) Ding, B.; Soblosky, L.; Nguyen, K.; Geng, J.; Yu, X.; Ramamoorthy, A.; Chen, Z. *Sci. Rep.* **2013**, *3*, 1854.
(59) Ye, S.; Nguyen, K. T.; Chen, Z. *J. Phys. Chem. B* **2010**, *114*, 3334−3340.
(60) Nguyen, K. T.; King, J. T.; Chen, Z. *J. Phys. Chem. B* **2010**, *114*, 8291−300.
(61) Fu, L.; Wang, Z.; Yan, E. C. Y. *Int. J. Mol. Sci.* **2011**, *12*, 9404−9425.
(62) Miyazawa, T. *J. Chem. Phys.* **1960**, *32*, 1647−1651.
(63) Sagle, L. B.; Cimatu, K.; Litosh, V. a; Liu, Y.; Flores, S. C.; Chen, X.; Yu, B.; Cremer, P. S. *J. Am. Chem. Soc.* **2011**, *133*, 18707−18712.
(64) Simpson, G. J.; Rowlen, K. L. *J. Am. Chem. Soc.* **1999**, *121*, 2635−2636.
(65) Ji, N.; Ostroverkhov, V.; Chen, C.-Y.; Shen, Y.-R. *J. Am. Chem. Soc.* **2007**, *129*, 10056−10057.
(66) Hu, D.; Chou, K. C. *J. Am. Chem. Soc.* **2014**, *136*, 15114−15117.
(67) Chen, X. K.; Hua, W.; Huang, Z. S.; Allen, H. C. *J. Am. Chem. Soc.* **2010**, *132*, 11336−11342.
(68) Panahi, A.; Brooks, C. L., III. *J. Phys. Chem. B* **2015**, *119*, 4601−4607.
(69) Roy, S.; Naka, T. L.; Hore, D. K. *J. Phys. Chem. C* **2013**, *117*, 24955−24966.
(70) Flavell, R. R.; Muir, T. W. *Acc. Chem. Res.* **2009**, *42*, 107−116.
(71) Wang, L.; Schultz, P. G. *Angew. Chem., Int. Ed.* **2004**, *44*, 34−66.
(72) Stiopkin, I. V.; Jayathilake, H. D.; Bordenyuk, A. N.; Benderskii, A. V. *J. Am. Chem. Soc.* **2008**, *130*, 2271−2275.
(73) Nihonyanagi, S.; Yamaguchi, S.; Tahara, T. *J. Chem. Phys.* **2009**, *130*, 204704.
(74) Xiong, W.; Laaser, J. E.; Mehlenbacher, R. D.; Zanni, M. T. *Proc. Natl. Acad. Sci. U. S. A.* **2011**, *108*, 20902−20907.
(75) Laaser, J. E.; Zanni, M. T. *J. Phys. Chem. A* **2013**, *117*, 5875−5890.
(76) Zhang, Z.; Piatkowski, L.; Bakker, H. J.; Bonn, M. *Nat. Chem.* **2011**, *3*, 888−893.

DOI: 10.1021/jacs.5b04024
J. Am. Chem. Soc. 2015, 137, 10190−10198